Liquid Crystals
Publication details, including instructions for authors and subscription information:
http://www.informaworld.com/smpp/title~content=t713926090

The in-plane switching of homogeneously aligned nematic liquid crystals

Masahito Oh-E; Katsumi Kondo

Online publication date: 06 August 2010

To cite this Article Oh-E, Masahito and Kondo, Katsumi(1997) 'The in-plane switching of homogeneously aligned nematic liquid crystals', Liquid Crystals, 22: 4, 379 — 390
To link to this Article: DOI: 10.1080/026782997209090
URL: http://dx.doi.org/10.1080/026782997209090

LIQUID CRYSTALS, 1997, VOL. 22, NO. 4, 379–390

The in-plane switching of homogeneously aligned nematic liquid crystals

by MASAHITO OH-E* and KATSUMI KONDO
Hitachi Research Laboratory, Hitachi, Ltd., 7-1-1 Ohmika-cho, Hitachi-shi, Ibaraki-ken, 319-12, Japan

(*Received 20 June 1996; accepted 24 October 1996*)

We have investigated the electro-optical effects and physical switching principle of homogeneously aligned nematic liquid crystals when applying an in-plane electric field with interdigital electrodes. By using the in-plane switching (IPS) of the liquid crystals which is achieved by the in-plane electric field, the viewing angle characteristics of the electro-optical effects were confirmed to be far superior to those of the conventional twisted nematic mode in which the electric field is applied along the direction perpendicular to the substrates. The non-reversal region of grey scales was extremely wide in which a high contrast ratio was kept, even along quite an oblique direction in the IPS mode. In order to clarify the switching principle of the liquid crystals in the IPS mode, a simplified expression describing the threshold behaviour of the device was derived with the assumption that a uniform in-plane electric field was applied along a direction perpendicular to the director and parallel to the homogeneously aligned nematic slab, and found to be sufficiently able to explain the experimental results. First, a critical field at which the liquid crystals just began to twist, was found to be proportional to the reciprocal of the cell gap. Second, it was the electric field and not the voltage that drives the liquid crystals. This relationship was due to the independence of the electric field regarding the liquid crystal layer normal direction. So the threshold voltage in the IPS mode was strongly dependent on the variation of the cell gap. For the dynamical response mechanism of the liquid crystals to the in-plane electric field, the switching on and off processes of the liquid crystals were analysed quantitatively. The relaxation time of the liquid crystals when removing the electric field could be described as proportional to the square of the cell gap. A thinner cell gap also proved to be effective in obtaining a fast response time in the IPS mode. In contrast, the switching on time when applying the in-plane electric field was found to be inversely proportional to the difference between the square of the electric field strength and the square of the critical electric field strength at which the liquid crystals began to deform.

1. Introduction

Many findings and investigations on electro-optical characteristics of liquid crystals have led to commercial uses of liquid crystals [1]. The electro-optical effects vary not only with the type and assembly structure of the liquid crystals, but also by how an electric field is applied to the liquid crystals. Twisted nematic (TN) and super-twisted nematic (STN) liquid crystals sandwiched by two substrates, which have transparent electrodes, have enjoyed much practical use [2, 3]. In these conventional modes, the contrast is obtained by the response of the liquid crystals to an electric field applied perpendicular to the substrates. The rising up movement of the liquid crystal molecules when changing from a twisted state to an untwisted state plays a part in the unstable electro-optical effects which are strongly dependent on the viewing angle. Due to the sensitivity of viewed optical characteristics to molecular orientation, the viewing angle is restricted. The variation of the electro-optical characteristics with the viewing angle direction is caused by variation of the birefringence effect. The birefringence effect induces asymmetric deformation profiles of the electro-optical characteristics from the viewing angles. TN devices, in particular, are widely employed for display applications using actively addressed driving techniques by thin film transistors because of their well-established production process and good performance qualities [4]. However, the strong viewing angle dependence of the contrast ratio, the grey scale and the brightness have been recognized as major weaknesses of these devices.

A variety of methods have been proposed as techniques for overcoming the limited viewing angle characteristics. As one possible replacement for TN devices, the guest–host mode was studied [5]. Despite the better

*Author for correspondence.
Present address: Electron Tube & Devices Division, Hitachi, Ltd., 3300 Hayano, Mobara-shi, Chiba-ken, 297 Japan.

0267–8292/97 $12·00

angular characteristics obtained by utilizing the guest–host mode, it was found that other performance qualities, such as contrast ratio and voltage retention time, were insufficient compared to TN devices. Another approach for optically improving the viewing angle characteristics of TN devices was proposed which used birefringence films [6–10]. At first, optical compensation by birefringence films was based on a normally black display mode, hence there were too many disadvantages, including low contrast ratio and poor colour reproduction owing to rotatory dispersion [6, 7]. The optical performance of the compensated, normally black, TN devices was still inferior to that of normally white TN devices. Subsequently, combinations of compensation films with normally white TN devices were presented [8, 9]. As a result, the optical performance of the dark state was significantly improved. However, light leakage in the dark state was not completely prevented because of the twist orientation structure of the liquid crystals near the alignment layer due to surface anchoring. To compensate 38for twist retardation near the alignment layer, an investigation of biaxial birefringence films was made and these new films have proved to be more effective than conventional birefringence films [10].

Nematic liquid crystals are characterized as an optically uniaxial medium. So, in a nematic slab, the birefringence effect cannot be neglected when the light is transmitted along an oblique direction. For this reason, ideas for gaining wide viewing angle characteristics must remove the birefringence effect by optical compensation. Multi-domain devices in which the liquid crystal alignment is divided among individual pixels are also based on optical compensation [11–19]. With the help of a function to average the transmission of each domain, the capability for wide viewing angle characteristics is possible. Yang [11, 12] proved that dividing each TN pixel into two domains improves the viewing angle characteristic because of the average effect of the electro-optical characteristics. With two domains, shifting the viewing location up or down yields the same reduction in the ratio of intensity between adjacent grey scales. The two-domain technique is implemented by different fabrication processes for the two domains in each pixel, i.e. by achieving a different rubbing direction in each pixel using a photoresist process [11–13] or by combination of high and low pretilt-angle alignment layers [14]. Tilted homeotropic devices have also been considered [15].

As the next developmental stage, amorphous [16] and four-domain [17] TN devices were proposed. In addition to the two-domain techniques, there are other fabrication routes to obtain four domains in each pixel. One utilizes the polarization of the polymerization of polyvinyl cinnamate films and the fact that a pretilt angle can be induced with oblique exposure [18]. In another method, one photolithographic step is required [19]. Using multi-domain devices led to improved reversal of grey scales, however, a decrease in the contrast ratio along the oblique direction could not be prevented which is due to light leakage from the increased transmission in the dark state. In addition, domain walls caused drops in the brightness and contrast ratio.

As another approach for solving the viewing angle problems, an electro-optical effect was considered which inherently has better symmetry properties. A pi-cell coupled with a negative birefringence film was found to provide a uniform grey scale performance as the viewing angles were varied [20–22]. Furthermore, an optically compensated bend (OCB) mode was proposed which was the combination of a bend structure of the liquid crystals with a birefringence film [23, 24]. The fundamental idea of the OCB mode is to stack three plates of uniaxial medium so that an effectively isotropic medium can be obtained. The bend structure of the liquid crystals functions as symmetric compensation along the normal direction to the liquid crystal layer. In addition to the wide viewing angle characteristics, the OCB mode shows better switching between grey scales in comparison to TN devices. Among optically compensated LCDs, the above mentioned multi-domain and OCB modes are candidates for wide viewing angle LCDs in the near future. However, multi-domain mode devices prove difficult in the manufacturing stage, and it is difficult to maintain stable control of liquid crystals using a bias voltage in the OCB mode.

In this paper, the IPS mode using nematic liquid crystals is reported as a novel possiblity for greatly improving the viewing angle characteristics. For the purpose of understanding the IPS mode, we analyse the switching principle and response mechanism of nematic liquid crystals governed by the in-plane electric field. The liquid crystals respond to an in-plane electric field while retaining the plane of the substrates in the IPS mode. To achieve this lateral switching of the liquid crystals, the electric field is provided along a direction parallel to the plane of the substrates with interdigital electrodes. From a historical viewpoint, interdigital electrodes, parallel strips shaped like a comb, were used in the early 1970s to apply an electric field to liquid crystals on both upper and lower substrates [25]. The dynamic scattering effect using interdigital electrodes formed only on lower substrates was reported [26] and the electro-optical effect of nematic liquid crystals with interdigital configuration was extended [27]. In the early 1990s a positive influence of the IPS mode on the viewing angle dependence was predicted by computer calculations [28–31]. However, significant physical phenomena concerned with the physical switching behaviour and the

response mechanism of the liquid crystals in the IPS mode have not been sufficiently clarified. We have already reported our success in combining the IPS mode and the actively addressed driving technique [32, 33], but, for practical use, it is necessary to analyse the physical behaviour of the liquid crystals which responds to the in-plane electric field [34–37]. The present paper also looks at the concept of the switching mechanism of the liquid crystals by the in-plane electric field.

We then report measurements of the electric-optical characteristics and analyses of the switching principles of the IPS mode. The physical switching behaviour of the liquid crystals governed by the in-plane electric field is analysed by using the continuum elastic theory. We experimentally confirmed the improvement of the viewing angle characteristics with the IPS mode. Finally, we discuss the dynamical response mechanism of the liquid crystals in the IPS mode from analytical and experimental viewpoints.

2. Experimental

2.1. *Preparation*

Samples for experiments were prepared by sandwiching liquid crystals between two rubbed polyimide coated substrates. Figure 1 shows a schematic cell structure for investigating the IPS effect. In order to apply the in-plane electric field to the liquid crystals, interdigital electrodes made of chromium were formed on one substrate and no electrodes were prepared on the other. The two substrates were set in the same rubbing direction to obtain homogeneously aligned liquid crystals. In order to prepare a uniform cell gap, polymer bead spacers were scattered over the lower substrate. The liquid crystal materials, ZLI-2806 and MLC-2011 (Merck KGaA, Darmstadt), which both exhibit the nematic phase at room temperature and negative dielectric anisotropy, were used; ZLI-2806 (nematic–isotropic temperature T_{NI}, 100°C; birefringence Δn, 0·0437 (20°C); dielectric anisotropy $\Delta\varepsilon$, −4·8 (20°C, 1 kHz); viscosity η, 57 cp (20°C) and MLC-2011 (nematic–isotropic temperature T_{NI}, 100°C; birefringence Δn, 0·0742 (20°C); dielectric anisotropy $\Delta\varepsilon$, −3·3 (20°C, 1 kHz); viscosity η, 18 cp (20°C)). For evaluating the viewing angle characteristics of TN mode, ZLI-3788 (Merck KGaA) was used; ZLI-3788 (nematic–isotropic temperature T_{NI}, 90°C; birefringence Δn, 0·1019 (20°C); dielectric anisotropy $\Delta\varepsilon$, +4·5 (20°C, 1 kHz); viscosity η, 18 cp (20°C)).

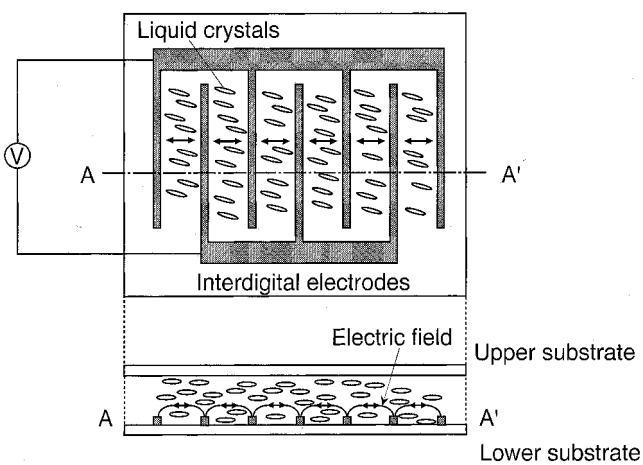

Figure 1. A schematic liquid crystal cell structure for an in-plane switching mode.

2.2. *Measurements*

The schematic diagram in figure 2 (*a*) shows the electro-optical measurement system used in our study. The electro-optical characteristics were measured by using a polarized microscope (Olympus BH-3) with a filter for brightness correction and a photomultiplier. Light transmitted through samples was detected with the photomultiplier as the desired voltage was applied to the samples. The polarizer and analyser were always set at right angles to the axes. The definition of the viewing angle direction was as described in figure 2 (*b*). Grey scales were determined as the voltages at which transmittances were 100%, 85·5%, 57·0%, 35·1%, 20·7%,

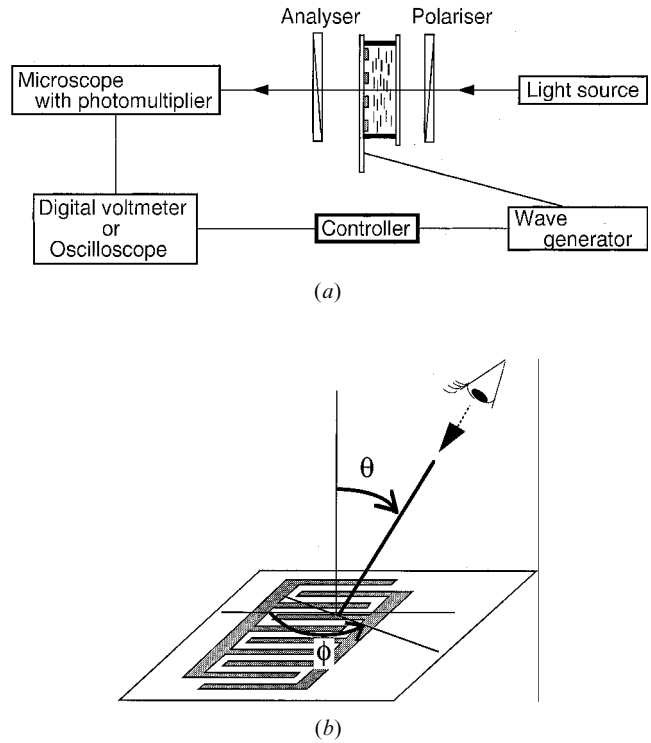

Figure 2. (*a*) A schematic diagram of the measurement system for electro-optical characteristics and (*b*) definition of the viewing angle direction.

11·2%, 4·6% and 1·0% from the front view, assuming the maximum transmittance was 100%.

The response time was measured from the signals triggered by switching a wave generator (Hewlett–Packard 8175A) on and off. The signals were observed with a digital oscilloscope (Hewlett–Packard 54110A). The response time was defined as the sum of the times from the moment of the switching on or off of the field to that at which a 90 per cent optical change from the off-state to the on-state or from the on-state to the off-state was achieved.

3. Results and discussion

3.1. *Threshold behaviour*

First of all, we measured the voltage-dependent optical transmittance for a variety of electrode distances. Figure 3 shows the electro-optical characteristics using ZLI-2806, a negative dielectro-anisotropic liquid crystal. In the IPS mode homogeneously aligned liquid crystals, for which the optical axis direction was in good agreement with the polarization axis of the analyser, formed a pure dark state in the absence of an electric field. This meant a pure modulation was achieved because the light behaved as an extraordinary ray. However, an in-plane electric field parallel to the plane of the substrate caused twist deformation of the liquid crystal layer. The liquid crystal molecules began to rotate and the liquid crystal director deviated from the polarization axis, as the electric field was applied. From an optical viewpoint, transmittance was gradually increased because phase retardation occurred due to the different propagating speed of the extraordinary and ordinary rays in the liquid crystal medium. Here the phase retardation was described as

$$\delta = \frac{2\pi d\Delta n(V, T, \lambda)}{\lambda} \qquad (1)$$

where d corresponds to the thickness of liquid crystal layer and $\Delta n(V, T, \lambda)$ denotes the effective liquid crystal birefringence which is dependent on applied voltage (V), temperature (T) and wavelength (λ) of incident light.

We use the theory of light transmission in a uniaxial medium to describe the transmitted light [38]. When the polarizer and analyser are placed in the configuration where the polarization axes are at right angles, the normalized transmission through the liquid crystal layer can be given by

$$T/T_0 = \sin^2(2\chi)\sin^2\left(\frac{\delta}{2}\right) = \sin^2(2\chi)\sin^2\left(\frac{\pi d\Delta n(\phi, \theta)}{\lambda}\right) \qquad (2)$$

where χ symbolises the angle between the effective optical axis of the liquid crystals and the polarization axis of incident light, and ϕ and θ are azimuthal and polar angles of the viewing direction. The birefringence Δn is dependent on the viewing direction, ϕ and θ. When the dark state is selected, the first sine term is zero in equation (2). When the bright state is selected as the angle χ equals 45°, equation (2) can be simplified to

$$T/T_0 = \sin^2\left(\frac{\delta}{2}\right) = \sin^2\left(\frac{\pi \mathrm{d}\Delta n(\phi, \theta)}{\lambda}\right). \qquad (3)$$

The experimentally obtained results of the voltage-dependent transmittance profiles (see figure 3) could be explained with the above theoretical equation. In the initial state in which there was no electric field, the direction of the optical axis in the liquid crystal layer was the same as that of the transmission axis of the polarizer and/or the polarization axis of the analyser. The configuration of the homogeneously aligned liquid crystals and the polarizer and analyser at right angles to each other played an important role in blocking the

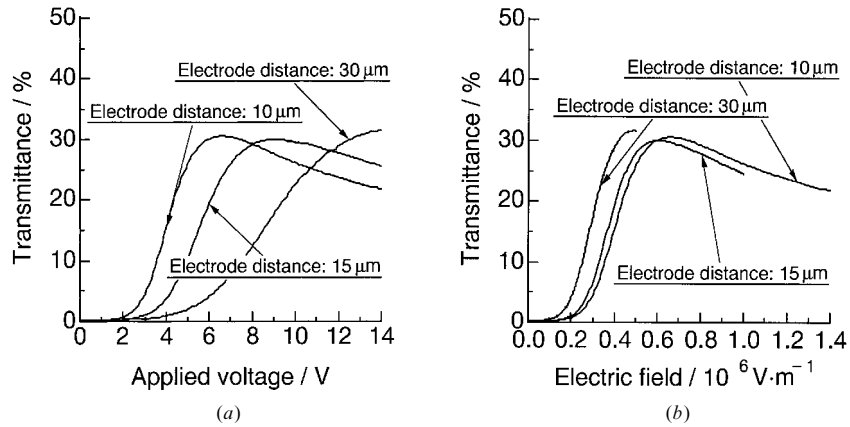

Figure 3. (*a*) Voltage and (*b*) electric field-dependent transmittance characteristics as a function of electrode distance. LC, ZLI-2806, interdigital electrode width, 10 μm, cell gap, 6·5 μm, temperature, 20°C.

light. By contrast, when the electric field was gradually applied to the liquid crystals, rotation of the optical axis in the plane of the substrates allowed the incident light to be transmitted, because the phase retardation was generated in the liquid crystal layer. The maximum transmittance meant the effective liquid crystal director twisted and was 45° from the transmission axis of the polarizer.

The brightness in the state at which the transmission was the maximum was then governed by the retardation in the liquid crystal layer. In order to get a brighter outgoing beam and higher contrast ratio, the following condition must be satisfied:

$$\frac{d\Delta n}{\lambda} = \left(m + \frac{1}{2}\right), \quad m = 0, 1, 2, \ldots \tag{4}$$

For an assumed incident light wavelength of 550 nm, it is appropriate to set the retardation $d\Delta n = 275$ nm, 825 nm, 1375 nm,..., corresponding to the zero, first, second,... birefringence modes, respectively. Here we chose the zero order birefringence mode, which corresponds to $m = 0$ in equation (4). The advantage of this choice is to be able to obtain the smallest possible optical transmittance dependence on the wavelength through the liquid crystals.

In order to understand how the switching mechanism of the liquid crystals is governed by the in-plane electric field, the continuum elastic theory [39] was used. We use it to suppose that the homogeneously aligned liquid crystals following the in-plane electric field are perpendicular to the liquid crystal director and, at the same time, parallel to the substrates. We then analyse the Freedericksz transition. Figure 4 illustratess the geometry of the twist deformation in the plane of the substrates by the in-plane electric field. Here we assumed the in-plane electric field was uniform throughout the nematic slab and the liquid crystals on the surface of the alignment layer were strongly anchored, i.e. $\phi(0) = \phi(d) = 0$. The electric field was applied along the y direction, which is parallel to the substrates and perpendicular to the director. For this geometry, the director vector of the liquid crystals, defined as $(1, 0, 0)$ in the state without the electric field, was expressed as $(\cos\phi(z), \sin\phi(z), 0)$. Assuming no current and space charge exist, the free energy F of twist deformation could be expressed as

$$F = \frac{1}{2}\int_0^d \left\{ K_2 \left(\frac{\mathrm{d}\phi}{\mathrm{d}z}\right)^2 - \varepsilon_0 |\Delta\varepsilon| E^2 \sin^2\phi \right\} \mathrm{d}z \tag{5}$$

where K_2 is the elastic constant of twist deformation, ϕ symbolises the twist angle, ε_0 is the vacuum dielectric constant, $\Delta\varepsilon$ denotes dielectric anisotropy and E corresponds to the electric field strength. The deformation involves only the twist modulus K_2.

By applying the Euler–Lagrange equation, the following equation was then obtained:

$$K_2 \frac{\mathrm{d}^2\phi}{\mathrm{d}z^2} + \varepsilon_0 |\Delta\varepsilon| E^2 \sin\phi\cos\phi = 0. \tag{6}$$

With the assumption that the twist angle ϕ was small and the boundary condition was $\phi(0) = \phi(d) = 0$, the solution of equation (6) could be reduced to

$$\left(\frac{\varepsilon_0 |\Delta\varepsilon|}{K_2}\right)^{1/2} Ed = m\pi. \tag{7}$$

In equation (7), $m = 0$ corresponds to the case with no electric field, and $m = 1$ means the critical field E_c at which the twist angle ϕ just begins to change.

$$E_c^{\mathrm{IPS}} = \frac{\pi}{d}\left(\frac{K_2}{\varepsilon_0 |\Delta\varepsilon|}\right)^{1/2}. \tag{8}$$

Deformation of the homogeneously aligned liquid crystals only occurs just above the critical field E_c. This equation is referred to as the Freedericksz effect. Thus, the threshold voltage V_c in the IPS mode can be expressed as

$$V_c^{\mathrm{IPS}} = E_c^{\mathrm{IPS}} \times l = \frac{\pi l}{d}\frac{K_2}{\varepsilon_0 |\Delta\varepsilon|} \tag{9}$$

where l is the electrode distance.

This equation predicts that the electrode distance determines the threshold voltage. However, at the same time the cell gap also influences the threshold behaviour. An anomalous relation V_c^{TN} is obtained in the case of the TN mode except for the elastic constant K_2 is replaced with K_1. By applying the electric field perpendicular to the plane of the substrates such as in the TN mode, the dependence of the electric field in a direction normal to the liquid crystal layer produces the threshold voltge, $V_c^{\mathrm{TN}} = E_c^{\mathrm{TN}} d$ in this case, because the electrode distance corresponds to the cell gap. Consequently, liquid crystals in the TN mode, for example, are driven by the voltage. By contrast, if the in-plane electric field parallel to the plane of the substrates for the IPS mode is considered ideally, then the electric field is independent

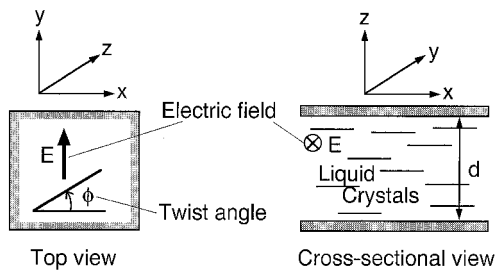

Figure 4. Geometry of twist deformation by an in-plane electric field.

of the liquid crystal layer normal direction. Therefore, liquid crystals are not governed by the voltage, but by the electric field itself in the IPS mode. Furthermore, the threshold voltage in the IPS mode seems changeable with variation of the cell gap. This was confirmed experimentally (see figure 5 (*a*)) that variation of the cell gap affects the threshold voltage. Then, as expected from equation (9), the reciprocal of the cell gap was shown to be proportional to the threshold voltage (see figure 5(*b*)).

In our experiment, the interdigital electrodes were much thinner than the nematic slab, which meant the horizontal electric field to the substrates was not complete. Figure 3 (*b*) shows the electric field-dependent optical transmittance measured with a variety of electrode distances. In figure 3 (*b*), the horizontal axis of the applied voltage in figure 3 (*a*) is replaced by the electric field strength. With a longer distance between the electrodes, the horizontal field component seems to be more effective. If it is not correct, the profiles in figure 3 (*b*) which show the electric field dependence of transmittance must be in good agreement with each other in spite of the different electrode distances. The findings show the experimental results can be analysed using the fact that the electro-optical characteristics change with variation of the cell gap, and the threshold voltage is proportional to the reciprocal of the cell gap. So the derived equation of the threshold voltage correctly expresses the switching behaviours of liquid crystals in the IPS mode.

3.2. *Viewing angle characteristics*

We evaluated viewing angle characteristics from the viewpoints of both grey scale reversal and contrast ratio. Figure 6 compares the viewing angle characteristics of the IPS mode and the TN mode in terms of grey scale reversal from all directions. The circular axis corresponds to the azimuthal direction ϕ and the crossed axes plot polar angle θ. The non-reversal region of grey scales when using the IPS mode is shown in figure 6 (*a*), and when using the TN mode is depicted in figure 6 (*b*). Comparing these plots, we felt better viewing angle characteristics could be expected with the IPS mode. No grey scale reversal was recognized even along quite an oblique direction in the IPS mode. The non-reversal region of grey scales was extremely wide, although small parts were left as grey scale reversal regions. By contrast, the TN mode was marked by a prominent turning around of grey scales in the oblique direction. The reason for the grey scale reversal in the TN mode was a rising up movement of the liquid crystal molecules due to the electric field applied perpendicular to the plane of the substrates. This behaviour of the liquid crystal molecules could bring about a strong birefringence dependence on the viewing angle direction. Meanwhile, the twisting movement of the liquid crystals, keeping them in the plane of the substrates, helped to maintain almost the same electro-optical behaviour along the oblique direction as in front of the cells. The small parts in which grey scale reversal was observed in the IPS mode, however, were in the same direction as longitudinal molecular axis driven by the in-plane electric field in a bright state.

It is possible to obtain no grey scale reversals in quite an oblique direction even by using methods other than the IPS mode, for example, the multi-domain mode. Retaining the higher contrast ratio along an oblique direction, however, has not been achieved with no grey scale reversal. The outstanding feature of the IPS mode is the capability of holding the high contrast ratio with no grey scale reversal at the same time. Figure 7 shows

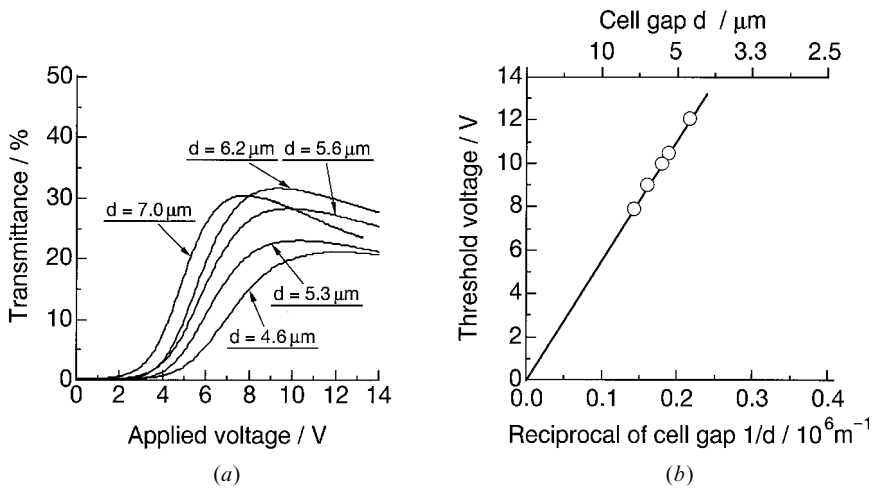

Figure 5. (*a*) Cell gap effects on voltage-dependent transmittance characteristics. (*b*) Relationship of the threshold voltage with the reciprocal of the cell gap. LC, ZLI-2806; interdigital electrode width, 10 μm, electrode distance, 15 μm, temperature, 20°C.

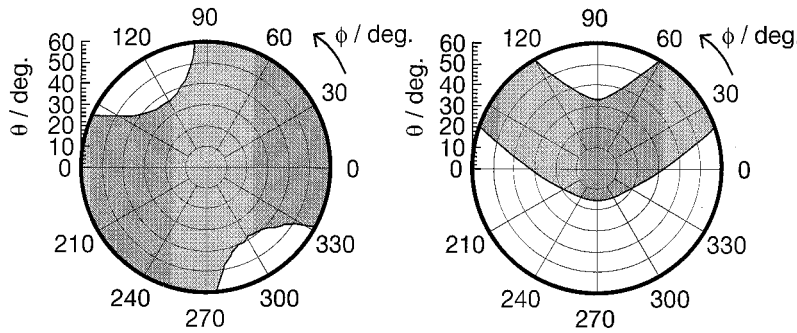

Figure 6. The non-reversal region of grey scales. (*a*) In the IPS mode. LC, ZLI-2806, interdigital electrode width, 10 μm, electrode distance, 15 μm, cell gap, 6·5 μm, temperature, 20°C. (*b*) In the TN mode. LC, ZLI-3788, cell gap, 5·3 μm, temperature, 20°C. Hatched regions correspond to the non-reversal region of grey scales.

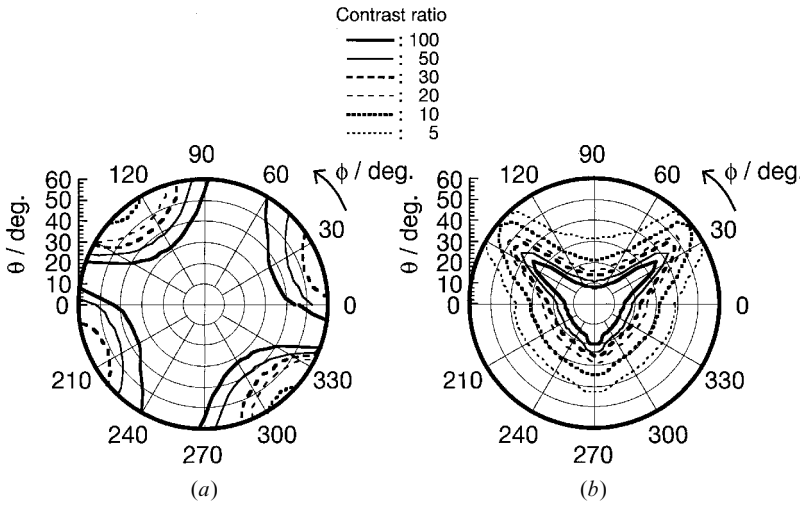

Figure 7. Contrast ratio dependence on viewing angle direction. (*a*) In the IPS mode. LC, ZLI-2806, interdigital electrode width, 10 μm, electrode distance, 15 μm, cell gap, 6·5 μm, temperature, 20°C. (*b*) In the TN mode. LC, ZLI-3788, cell gap, 5·3 μm, temperature, 20°C.

the contrast ratio dependence on the viewing angles for the IPS and TN modes. A higher contrast ratio was maintained, even along quite an oblique direction, with the IPS mode, whereas in the TN mode an abrupt decrease of the contrast ratio was recognizable. These features of the viewing angle characteristics could be caused by the way the modes generate the dark state. The combination of the TN configuration and the electric field perpendicular to the substrates causes a switching of the optical function between the rotatory power effect at a lower voltage and the birefringence effect due to the uniaxial media at a higher voltage. With a higher voltage, the orientation of the longitudinal axis becomes nearly perpendicular to the substrates. This behaviour corresponds to the fact that there is only one direction, which is nearly in front of the substrates, where the retardation is equal to zero. This means that the completely dark state can be obtained only when the viewing angle direction is perpendicular to the substrates. In general, since the angle χ in equation (2) is non-zero, the inclined incident light passes through due to the non-zero retardation term. This problem may be observed even when each pixel is divided into sub-pixels. On the other hand, in the IPS mode, the first sine term of equation (2) is zero in the dark state, that is to say, the optical axis direction of the liquid crystals is in good agreement with the polarization axis of the polarizer. Therefore a pure dark state is generated by two crossed polarizers, which is not affected by the birefringence of the liquid crystal layer. In the TN mode, however, the optical path difference along the direction perpendicular to the plane of the substrate is strongly related to generation of the dark state, which is strongly dependent on the viewing angle direction, because the birefringence Δn is dependent on the viewing direction, ϕ and θ. In the IPS mode, the excellent viewing angle

characteristics lie in the fact that the switching from the dark state to the bright state is achieved by the switching of the first sine term in equation (2). The well-functioned light blocking, which is insensitive to the viewing angle direction, generates extremely wide viewing angle characteristics.

3.3. *Dynamical response mechanism*

In static deformation of liquid crystal directors, a balance equation is described by elastic torque and electric torque exerted by the applied electric field. By contrast, for dynamical responses, the viscous torque, which opposes the director rotation, should be included [39, 40]. It is well known that the Erickson–Leslie expression [41, 42] can be used for describing the dynamics of the liquid crystal director rotation. Moreover, under the condition of neglecting backflow and inertial effects, this equation can be simplified to a torque balance equation. Switching on and off times of the liquid crystals in the IPS mode are also derived with an equilibrium equation in which the elastic, electric and viscous torques are expressed as:

$$\gamma_1 \frac{\partial \phi}{\partial t} = K_2 \frac{\partial^2 \phi}{\partial z^2} + \varepsilon_0 |\Delta\varepsilon| E^2 \sin\phi \cos\phi \qquad (10)$$

where γ_1 is the twist-viscous coefficient. To simplify the analysis, we assumed the anchoring strength of the surface of the polymer which aligns the liquid crystal molecules is strong, i.e. $\phi(0) = \phi(d) = 0$, and the degree of the twist deformation at the centre of the liquid crystal layer is the largest, i.e. $\phi(d/2) = \phi_m$. So using the condition, $\phi(0) = \phi(d) = 0$ and $\phi(d/2) = \phi_m$, the description of twist angle ϕ along z direction could be expressed as:

$$\phi_0(z) = \phi_m \sin\left(\frac{\pi z}{d}\right). \qquad (11)$$

First we considered the case in which the electric field is removed at time $t = 0$. The relaxation time τ for returning from the state at which the electric field is applied to the initial state of the liquid crystals can be expressed by using the function $\phi(z, t) = \phi_0(z) \exp(-t/\tau)$:

$$\tau_{off} = \frac{\gamma_1 d^2}{\pi^2 K_2} = \frac{\gamma_1}{\varepsilon_0 |\Delta\varepsilon| E_c^2}. \qquad (12)$$

This derived equation indicates that the switching off time is governed by the twist-viscous term divided by the elastic property which is related to a restoring force. Furthermore, the cell gap is one of the factors that determine the switching off time. A thinner cell gap is expected to make a large elastic energy behave as the restoring force and contribute to a fast response time as well as provide low viscous and large elastic properties. Figure 8 displays the cell gap effect on the switching off process. The liquid crystal material used in this experiment was ZLI-2806 which has a negative dielectric anisotropy. As expected from the theoretical consideration, we confirmed that the relaxation time of the switching off process is proportional to the square of the cell gap. A thinner cell gap between substrates has the advantage of faster switching off times of the liquid crystals in the IPS mode.

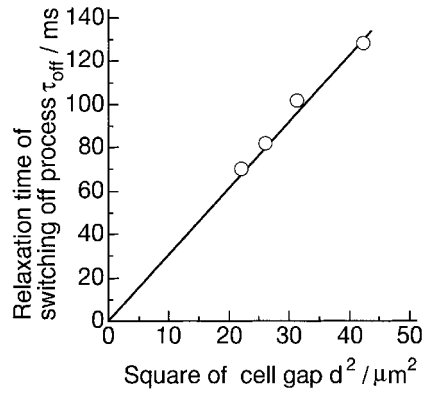

Figure 8. Relationship between the relaxation time of the liquid crystals when removing an in-plane electric field and the cell gap. LC, ZLI-2806, interdigital electrode width, 10 μm, electrode distance, 15 μm, temperature, 20°C.

Next we analysed the switching on process. Under the assumption that the deformation of the twist angle ϕ was small, the torque balance equation (10) could be simplified to

$$\gamma_1 \frac{\partial \phi}{\partial t} = K_2 \frac{\partial^2 \phi}{\partial z^2} + \varepsilon_0 |\Delta\varepsilon| E^2 \phi. \qquad (13)$$

Then solving this equation for the response time for the switching on process as follows:

$$\tau_{on} = \frac{\gamma_1}{\varepsilon_0 |\Delta\varepsilon| E^2 - \frac{\pi^2}{d^2} K_2} = \frac{\gamma_1}{\varepsilon_0 |\Delta\varepsilon| (E^2 - E_c^2)}, \qquad (14)$$

$$\frac{1}{\tau_{on}} = \frac{\varepsilon_0 |\Delta\varepsilon| (E^2 - E_c^2)}{\gamma_1}. \qquad (15)$$

As explained by equation (14), the switching on time is expressed by the twist-viscous coefficient divided by the term consisting of the electric field term and the elastic constant. However, the denominator can be transformed into the subtraction of the square of the critical field from the square of the field strength. The switching on time seems to be strongly dependent on the electric field strength in addition to the twist viscous coefficient. In order to understand the effect of the field strength on the switching on time, the relationship of $1/\tau_{on}$ with $(E^2 - E_c^2)$ was analysed. These experimental results are shown in figure 9, which indicates there is a proportional

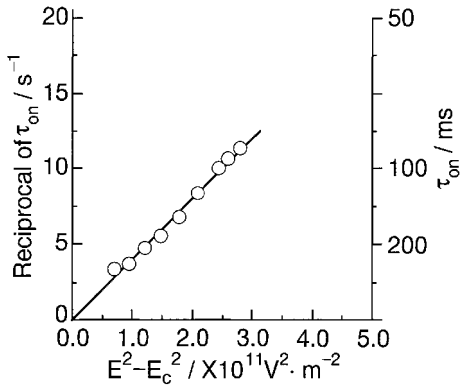

Figure 9. Relationship between the relaxation time of the liquid crystals when applying an in-plane electric field and the electric field strength. LC, ZLI-2806, interdigital electrode width, 10 μm, electrode distance, 15 μm, cell gap, 6·5 μm, temperature, 20°C.

relationship of the reciprocal of relaxation time τ_{on} in the switching on process with the difference between the square of the electric field strength and the square of the critical field ($E^2 - E_c^2$). Thus, the response time for the switching on process is strongly dependent on the electric field strength.

The expressions that explain the switching on and off times in the IPS mode as in the TN mode suggest that the elastic energy is significant for determining response time. This elastic energy is in the layer thickness of the liquid crystals. It it is assumed that the same degree of twist deformation occurs in the layer, a larger elastic energy should exist in a thinner liquid crystal layer than in a thicker layer. However, the fact that the response time is not actually dependent on the electrode distance in the IPS mode may cause some confusion. Even if the electrode distance is reduced, a faster response time cannot be expected because it is the electric field and not the voltage that the liquid crystals respond to. If the electrode distance is reduced, the critical voltage will be decreased but the critical electric field cannot be changed. It is the reduced cell gap and not the electrode distance which shortens the response time in the IPS mode. Therefore, both the switching on time and switching off time are independent of the electrode distance.

The response time in the IPS mode seems to be potentially slower than in the TN mode. In fact, we could not obtain an IPS mode response time equivalent to a TN mode response time. Figure 10 (*a*) shows the voltage-dependent transmittance using ZLI-2806. Figure 10 (*b*) displays the corresponding voltage-dependent response time. The response time for the sum of the switching on and off times at the maximum transmittance was over 300 ms. However, an IPS mode response time equivalent to a TN mode could be achieved by using the above-mentioned analysis of the

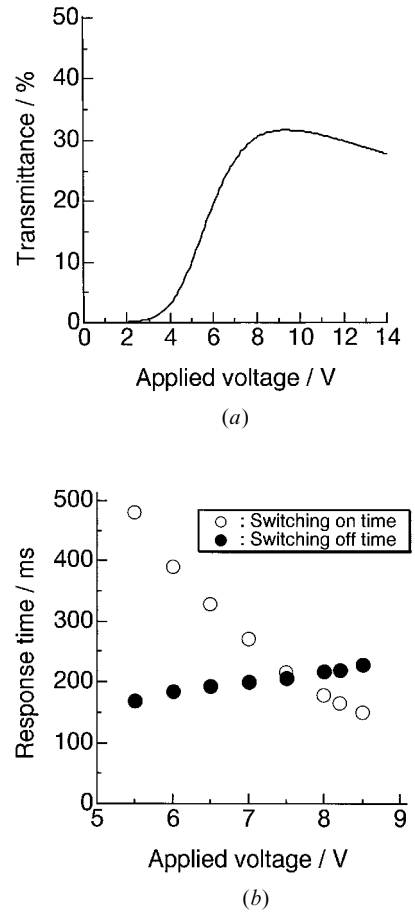

Figure 10. (*a*) Voltage-dependent transmittance using the liquid crystal, ZLI-2806. (*b*) Corresponding voltage-dependent response time in the switching on and off processes. Interdigital electrode width, 10 μm, electrode distance, 15 μm, cell gap, 6·5 μm, temperature, 20°C.

response time and optimizing the cell gap. In order to set a thinner cell group which is favourable to the faster response time, a relatively large birefringence liquid crystal material was selected. Figure 11 (*a*) shows the voltage-dependent transmittance using MLC-2011. Figure 11 (*b*) displays the corresponding voltage-dependent response time. The cell gap was set to 4·0 μm in order to optimize the optical difference of the liquid crystal layer. As expected, the response time between the off and on states was significantly improved by using this material. Although it was certain that the lower viscosity of the liquid crystal contributed to the faster response time, the substantial improvement could not be explained without the thinner cell gap. In the case of ZLI-2086, the relaxation time of the switching off process was 128·0 ms (cell gap: 6·5 μm). The relaxation time of the switching off process for MLC-2011 was 13·2 ms (cell gap: 4·0 μm), about 10 per cent of that of ZLI-2806. So

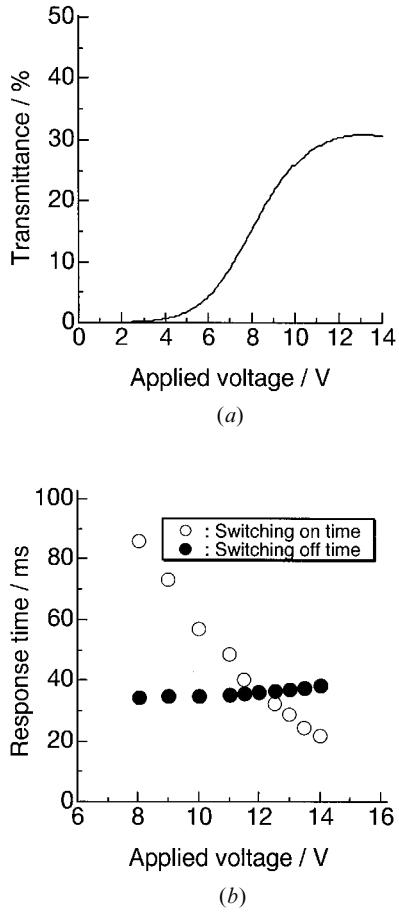

Figure 11. (*a*) Voltage-dependent transmittance using the liquid crystal, MLC-2011. (*b*) Corresponding voltage-dependent response time in the switching on and off processes. Interdigital electrode width, 10 μm, electrode distance, 15 μm, cell gap, 4·0 μm, temperature, 20°C.

by lowering the viscosity by about 32 per cent, the relaxation time of the switching off process decreased. Thus we concluded that the remaining improvement was attributable to the thinner cell gap. This improvement of about 10 per cent was in good agreement with the per cent-ratio of the square of the cell gaps multiplied by the per cent change in viscosity. Furthermore, the results of the response time measurements indicated that the switching off time was nearly independent of the electric field, while the switching on time depended on the strength of the electric field.

4. Conclusions

In conclusion, we analysed the electro-optical effects and the switching principle of nematic liquid crystals using the IPS mode. The most outstanding features of the IPS mode are the capability to show stable electro-optical effects even along quite an oblique direction and to provide extremely wide viewing angle characteristics. Experimentally the non-reversal region of grey scales was found to be very wide and no abrupt decrease of the contrast ratio occurred even along quite an oblique direction.

For the switching principle in the IPS mode, simplified theoretical expressions, which were derived with an assumption that an in-plane electric field was applied to the liquid crystals, were used to explain the threshold behaviour and the dynamical switching process. In this mode, the liquid crystals were driven not by the voltage but by the electric field. This distinctive behaviour was found to be due to the independence of the direction of the liquid crystal layer normal on the electric field direction. In addition, the critical field of the liquid crystals was shown to be inversely proportional to the cell gap between the substrates.

As for the response mechanism of the liquid crystals in the IPS mode, the relaxation time of the liquid crystals when removing the electric field was described as proportional to the square of the cell gap. A thinner cell gap also proved to be effective in obtaining a faster response time in the IPS mode. In contrast, the switching on time when applying the in-plane electric field was inversely proportional to the difference between the square of the electric field strength and the square of the critical electric field strength at which the liquid crystals begin to deform.

We wish to thank Mr M. Ohta for research into driving methods of the IPS mode. We are especially grateful to Dr S. Oh-hara of the Hitachi Research Laboratory for his encouragement. Gratitude is also extended to Mr H. Kawakami, Mr K. Kinugawa and Mr N. Konishi of the Electron Tube & Devices Division of Hitachi, Ltd for their support of this research.

References

[1] See for example: (*a*) Heilmeier, G. H., Zanoni, L. A., and Barton, L. A., 1968, *Appl. Phys. Lett.*, **13,** 46; (*b*) Heilmeier, G. H., and Zanoni, L. A., 1968, *Appl. Phys. Lett.*, **13,** 91; (*c*) Schadt, M., and Helfrich, W., 1971, *Appl. Phys. Lett.*, **18,** 127; (*d*) Schiekel, M. F., and Fahrenshon, K., 1971, *Appl. Phys. Lett.*, **19,** 391; (*e*) Grinberg, J., Jacobson, A., Bleha, W. P., Miller, L., Fraas, L., Bosewell, D., and Meyer, G., 1975, *Opt. Eng.*, **14,** 217; (*f*) Clark, N. A., and Lagerwall, S. T., 1980, *Appl. Phys. Lett.*, **36,** 899; (*g*) Bos, P. J., and Koehler, K. R., 1984, *Mol. Cryst. liq. Cryst.*, **113,** 329; (*h*) Scheffer, T. J., and Nehring, J., 1984, *Appl. Phys. Lett.*, **45,** 1021; (*i*) Scheffer, T. J., and Nehring, J., 1985, *J. appl. Phys.*, **58,** 3022; (*j*) Mochizuki, A., Gondo, H., Watanula, T., Saito, K., Ikegami, K., and Okuyama, H., 1985, Digest of Technical Papers of the 1985 Society for Information

Display International Symposium (Society for Information Display, Orlando), p. 135; (*k*) FERGASON, J. L., 1985, Digest of Technical Papers of the 1985 Society for Information Display International Symposium (Society for Information Display, Orlando), p. 68; (*l*) DOANE, J. W., VAZ, N. A., WU, B. G., and ZUMER, S., 1986, *Appl. Phys. Lett.*, **48,** 269; (*m*) KINUGAWA, K., KANDO, Y., KANASAKI, M., KAWAKAMI, H., and KANEKO, E., 1986, Digest of Technical Papers of the 1986 Society for Information Display International Symposium (Society for Information Display, San Diego), p. 122; (*n*) SCHADT, M., and LEENHOUTS, F., 1987, *Appl. Phys. Lett.*, **50,** 236; (*o*) COLES, H. J., GLEESON, H. F., and KANG, J. S., 1989, *Liq. Cryst.*, **5,** 1243.

[2] SCHADT, M., and HELFRICH, W., 1971, *Appl. Phys. Lett.*, **18,** 127.

[3] SCHEFFER, T. J., and NEHRING, J., 1984, *Appl. Phys. Lett.*, **45,** 1021.

[4] See for example: LECOMBER *et al.*, 1979, *Electr. Lett.*, **15,** 179.

[5] See for example: (*a*) WHITE, D. L., and TALOR, G. N., 1974, *J. appl. Phys.*, **45,** 4718; (*b*) UCHIDA, T., SEKI, H., SHISHIDO, C., and WADA, M., 1981, Proceedings of the Society for Information Display, **22,** 41.

[6] YOSHIDA, H., NAKAMURA, K., OHASHI, M., TOMITA, I., and OKABE, M., 1991, Digest of Technical Papers of the 1991 Society for Information Display International Symposium (Society for Information Display, Anaheim), p. 590.

[7] YAMAGISHI, N., WATANABE, H., and YOKOYAMA, K., 1989, Proceedings of the 9th International Display Research Conference (Society for Information Display and the Institute of Television Engineers of Japan, Kyoto), p. 316.

[8] ONG, H. L., 1992, Proceedings of the 12th International Display Research Conference (Society for Information Display and the Institute of Television Engineers of Japan, Hiroshima), p. 247.

[9] HATOH, H., ISHIKAWA, M., HIRATA, J., HISATAKE, Y., and YAMAMOTO, T., 1992, *Appl. Phys. Lett.*, **60,** 1806.

[10] KUBOTA, H., TSUKANE, M., and ISHIHARA, S., 1995, Proceedings of the 15th International Display Research Conference (Society for Information Display and the Institute of Television Engineers of Japan, Hamamatsu), p. 127.

[11] YANG, K. H., 1991, Proceedings of the 11th International Display Research Conference (Society for Information Display, San Diego), p. 68.

[12] YANG, K. H., 1992, *Jpn. J. appl. Phys.*, **31,** L1603.

[13] TAKATORI, K., 1992, Proceedings of the 12th International Display Research Conference (Society for Information Display, Hiroshima), p. 594.

[14] KOIKE, Y., KAMADA, T., OKAMOTO, K., OHASHI, M., TOMITA, I., and OKABE, M., 1992, Digest of Technical Papers of the 1992 Society for Information Display International Symposium (Society for Information Display, Boston), p. 798.

[15] YAMAMOTO, T., HIROSE, S., CLERC, J. F., KONDO, Y., YAMAGUCHI, S., and AIZAWA, M., 1991, Digest of Technical Papers of the 1991 Society for Information Display International Symposium (Society for Information Display, Anaheim), p. 762.

[16] TOKO, Y., SUGIYAMA, T., KATOH, K., IIMURA, Y., and KOBAYASHI, S., 1993, *J. appl. Phys.*, **74,** 2071.

[17] SUGIYAMA, T., TOKO, Y., HASHIMOTO, T., KATOH, K., IIMURA, Y., and KOBAYASHI, S., 1994, Digest of Technical Papers of the 1994 Society for Information Display International Symposium (Society for Information Display, San Jose), p. 919.

[18] HASHIMOTO, T., SUGIYAMA, T., KATOH, K., SAITO, T., SUZUKI, H., IIMURA, Y., and KOBAYASHI, S., 1995, Digest of Technical Papers of the 1995 Society for Information Display International Symposium (Society for Information Display, Orlando), p. 877.

[19] CHEN, J., BOS, P. J., BRYANT, D. R., JOHNSON, D. L., JAMAL, S. H., and KELLY, J. K., 1995, Digest of Technical Papers of the 1995 Society for Information Display International Symposium (Society for Information Display, Orlando), p. 865.

[20] BOS, P. J., JOHNSON, P., and KOEHLER, R., 1983, Digest of Technical Papers of the 1983 Society for Information Display International Symposium (Society for Information Display, Philadelphia), p. 30.

[21] BOS, P. J., and KOEHLER, K. R., 1984, *Mol. Cryst. liq. Cryst.*, **113,** 329.

[22] BOS, P. J., and RAHMAN, J. A., 1993, Digest of Technical Papers of the 1993 Society for Information Display International Symposium (Society for Information Display, Seattle), p. 273.

[23] YAMAGUCHI, Y., MIYASHITA, T., and UCHIDA, T., 1993, Digest of Technical Papers of the 1993 Society for Information Display International Symposium (Society for Information Display, Seattle), p. 277.

[24] MIYASHITA, T., YAMAGUCHI, Y., and UCHIDA, T., 1995, *Jpn. J. appl. Phys.*, **34,** L117.

[25] SHIMOJYO, T., 1973, Proceedings of the Society for Information Display, **14,** 110.

[26] KOBAYASHI, S., 1972, Digest of Technical Papers of the 1972 Society for Information Display International Symposium (Society for Information Display, San Francisco), p. 68.

[27] SOREF, R. A., 1974, *J. appl. Phys.*, **45,** 5466.

[28] KIEFER, R., WEBER, B., WINDSCHEID, F., and BAUR, G., 1992, Proceedings of the 12th International Display Research Conference (Society for Information Display and the Institute of Television Engineers of Japan, Hiroshima), p. 547.

[29] BAUR, G., 1993, Freiburger Arbeitstagung Flussigkristalle, Abstract No. 22.

[30] BAUR, G., 1994, Freiburger Arbeitstagung Flussigkristalle, Abstract No. 23.

[31] BAUR, G., KAMM, M., KLAUSMANN, H., WEBER, B., WIEBER, B., and WINDSCHEID, F., 1994, 15th International Liquid Crystal Conference, Abstract No. K-P15 (Budapest).

[32] OH-E, M., OHTA, M., ARATANI, S., and KONDO, K., 1995, Proceedings of the 15th International Display Research Conference (Society for Information Display and the Institute of Television Engineers of Japan, Hamamatsu), p. 577.

[33] OHTA, M., OH-E, M., and KONDO, K., 1995, Proceedings of the 15th International Display Research Conference (Society for Information Display and the Institute of Television Engineers of Japan, Hamamatsu), p. 707.

[34] OH-E, M., OHTA, M., KONDO, K., and OH-HARA, S., 1994, 15th International Liquid Crystal Conference, Abstract No. K-P17 (Budapest).

[35] OH-E, M., and KONDO, K., 1995, *Appl. Phys. Lett.*, **67,** 3895.

[36] Oh-e, M., Ohta, M., and Kondo, K., 1996, Freiburger Arbeitstagung Flussigkristalle, Abstract No. 25 (Freiburg).
[37] Oh-e, M., and Kondo, K., 1996, *Appl. Phys. Lett.*, **69,** 623.
[38] Born, M., and Wolf, E., 1980, *Principles of Optics* (Pergamon Press, New York).
[39] de Gennes, P. G., 1974, *The Physics of Liquid Crystals* (Oxford Univ. Press, London).
[40] Jakeman, E., and Raynes, E. P., 1972, *Phys. Lett.*, **39A,** 69.
[41] Erickson, J. L., 1961, *Trans. Soc. Rheol.*, **5,** 23.
[42] Leslie, F. M., 1968, *Arch. Ration. Mechan. Anal.*, **28,** 265.